Proceedings of ALGORITMY 2012
pp. 22–31

ON NUMERICAL SIMULATION OF AIRFOIL VIBRATIONS INDUCED BY COMPRESSIBLE FLOW*

MILOSLAV FEISTAUER † AND JAN ČESENEK‡

Abstract. The subject of the paper is the numerical simulation of the interaction of two-dimensional compressible viscous flow and a vibrating airfoil. The airfoil is considered as a solid body with two degrees of freedom, moving in the vertical direction and rotating around an elastic axis. The numerical simulation consists of the solution of the Navier-Stokes system by the space discontinuous Galerkin method combined with BDF in time, coupled with a system of nonlinear ordinary differential equations describing the airfoil motion. The time-dependent computational domain and a moving grid are taken into account by the arbitrary Lagrangian-Eulerian (ALE) formulation of the Navier-Stokes equations. The applicability of the developed method is demonstrated by numerical experiments.

Key words. aeroelasticity, compressible Navier-Stokes equations, Arbitrary Lagrangian-Eulerian formulation, discontinuous Galerkin method, BDF method, flow induced airfoil vibrations

AMS subject classifications. 65M12, 65M60, 74F10, 76M10, 76M25

1. Introduction. The interaction between flowing fluids and vibrating structures is the main subject of aeroelasticity, which studies the influence of aerodynamic and elastic forces on an elastic structure. The flow-induced vibrations may affect negatively the operation and stability of the systems. Therefore, one of the main goals of aeroelasticity is the prediction and cure of the aeroelastic instability. This discipline achieved many results, particularly from engineering point of view (see, e.g. the monographs [1], [5] and [10]).

In our paper we are concerned with the numerical solution of airfoil vibrations induced by compressible viscous flow. The airfoil is considered as a solid flexibly supported body with two degrees of freedom, allowing its vertical and torsional oscillations. The airfoil vibrations are described by a system of second-order nonlinear ordinary differential equations for the vertical displacement of the airfoil and the rotation angle of the airfoil around its elastic axis. This system is discretized by the Runge-Kutta method and coupled with the numerical approximation of the compressible Navier-Stokes system written in the arbitrary Lagrangian-Eulerian (ALE) form. It is discretized by the discontinuous Galerkin finite element method (DGFEM) in space and the backward difference formula (BDF) in time. We give here a detailed description of all ingredients of the coupled fluid-structure interaction problem. The presented results of numerical experiments demonstrate the applicability of the developed method.

2. Formulation of the flow problem. We consider compressible flow in a bounded domain $\Omega_t \subset I\!R^2$ depending on time $t \in [0,T]$. We assume that the boundary of Ω_t is formed by three disjoint parts: $\partial\Omega_t = \Gamma_I \cup \Gamma_O \cup \Gamma_{W_t}$, where Γ_I is the inlet, Γ_O is the outlet and Γ_{W_t} denotes the boundary of an airfoil moving in dependence

*This work was supported by the Grant No. 201/08/0012 of the Czech Science Foundation.

†Charles University Prague, Faculty of Mathematics and Physics, Sokolovská 83, 186 75 Praha 8, Czech Republic (feist@karlin.mff.cuni.cz).

‡(jan.cessa@seznam.cz)

on time. The time dependence of the domain Ω_t is taken into account with the use of the *arbitrary Lagrangian-Eulerian* (ALE) method, see e.g. [11]. It is based on a regular one-to-one ALE mapping of the reference configuration Ω_0 onto the current configuration Ω_t: $\mathcal{A}_t : \overline{\Omega}_0 \longrightarrow \overline{\Omega}_t$, *i.e.* $\boldsymbol{X} \in \overline{\Omega}_0 \longmapsto \boldsymbol{x} = \boldsymbol{x}(\boldsymbol{X}, t) = \mathcal{A}_t(\boldsymbol{X}) \in \overline{\Omega}_t$. We define the domain velocity $\boldsymbol{z} = (z_1, z_2)$ defined by the relations $\tilde{\boldsymbol{z}}(\boldsymbol{X}, t) = \frac{\partial}{\partial t}\mathcal{A}_t(\boldsymbol{X})$, $t \in [0, T]$, $\boldsymbol{X} \in \Omega_0, \boldsymbol{z}(\boldsymbol{x}, t) = \tilde{\boldsymbol{z}}(\mathcal{A}^{-1}(\boldsymbol{x}), t)$, $t \in [0, T]$, $\boldsymbol{x} \in \Omega_t$, and the ALE derivative of a vector function $\boldsymbol{w} = \boldsymbol{w}(\boldsymbol{x}, t)$ defined for $\boldsymbol{x} \in \Omega_t$ and $t \in [0, T]$: $\frac{D^A}{Dt}\boldsymbol{w}(\boldsymbol{x}, t) = \frac{\partial \tilde{\boldsymbol{w}}}{\partial t}(\boldsymbol{X}, t)$, where $\tilde{\boldsymbol{w}}(\boldsymbol{X}, t) = \boldsymbol{w}(\mathcal{A}_t(\boldsymbol{X}), t)$, $\boldsymbol{X} \in \Omega_0$, $\boldsymbol{x} = \mathcal{A}_t(\boldsymbol{X})$. Then the system describing the compressible flow, which consists of the continuity equation, the Navier-Stokes equations and the energy equation (cf. [7]) can be written in the ALE form (see, e.g. [8])

$$\frac{D^A \boldsymbol{w}}{Dt} + \sum_{s=1}^{2} \frac{\partial \boldsymbol{g}_s(\boldsymbol{w})}{\partial x_s} + \boldsymbol{w}\, \mathrm{div}\boldsymbol{z} = \sum_{s=1}^{2} \frac{\partial \boldsymbol{R}_s(\boldsymbol{w}, \nabla \boldsymbol{w})}{\partial x_s}. \tag{2.1}$$

Here $\boldsymbol{w} = (w_1, \dots, w_4)^T = (\rho, \rho v_1, \rho v_2, E)^T \in \mathbb{R}^4, \boldsymbol{w} = \boldsymbol{w}(x, t)$, $x \in \Omega_t$, $t \in (0, T), \boldsymbol{g}_s(\boldsymbol{w}) = \boldsymbol{f}_s(\boldsymbol{w}) - z_s \boldsymbol{w}, \boldsymbol{f}_i(\boldsymbol{w}) = (\rho v_i, \rho v_1 v_i + \delta_{1i}\, p, \rho v_2 v_i + \delta_{2i}\, p, (E + p) v_i)^T$, $\boldsymbol{R}_i(\boldsymbol{w}, \nabla \boldsymbol{w}) = \left(0, \tau^V_{i1}, \tau^V_{i2}, \tau^V_{i1}\, v_1 + \tau^V_{i2}\, v_2 + k\partial\theta/\partial x_i\right)^T, \tau^V_{ij} = \lambda\, \mathrm{div}\boldsymbol{v}\, \delta_{ij} + 2\mu\, d_{ij}(\boldsymbol{v})$, $d_{ij}(\boldsymbol{v}) = (\partial v_i/\partial x_j + \partial v_j/\partial x_i)/2$.

We use the following notation: ρ – density, p – pressure, E – total energy, $\boldsymbol{v} = (v_1, v_2)$ – velocity, θ – absolute temperature, $\gamma > 1$ – Poisson adiabatic constant, $c_v > 0$ – specific heat at constant volume, $\mu > 0, \lambda = -2\mu/3$ – viscosity coefficients, k – heat conduction, τ^V_{ij} – components of the viscous part of the stress tensor, δ_{ij} – Kronecker symbol. The vector-valued function $\boldsymbol{w}$ is called the state vector, the functions $\boldsymbol{f}_i$ are the so-called inviscid fluxes and $\boldsymbol{R}_i$ represent viscous terms.

The above system is completed by the thermodynamical relations

$$p = (\gamma - 1)(E - \rho|\boldsymbol{v}|^2/2), \quad \theta = (E/\rho - |\boldsymbol{v}|^2/2)/c_v, \tag{2.2}$$

and is equipped with the initial condition $\boldsymbol{w}(x, 0) = \boldsymbol{w}^0(x)$, $x \in \Omega_0$, and the following boundary conditions:

$$\begin{aligned}
&\text{a)}\ \ \rho|_{\Gamma_I} = \rho_D, \quad \text{b)}\ \ \boldsymbol{v}|_{\Gamma_I} = \boldsymbol{v}_D = (v_{D1}, v_{D2})^{\mathrm{T}}, \\
&\text{c)}\ \ \sum_{i,j=1}^{2} \tau^V_{ij} n_i v_j + k\frac{\partial \theta}{\partial n} = 0 \quad \text{on } \Gamma_I, \\
&\text{d)}\ \ \boldsymbol{v}|_{\Gamma_{W_t}} = \boldsymbol{z}_D = \text{velocity of a moving wall}, \ \ \text{e)}\ \ \frac{\partial \theta}{\partial n}|_{\Gamma_{W_t}} = 0 \text{ on } \Gamma_{W_t}, \\
&\text{f)}\ \ \sum_{i=1}^{2} \tau^V_{ij} n_i = 0, \quad j = 1, 2, \quad \text{g)}\ \ \frac{\partial \theta}{\partial n} = 0 \text{ on } \Gamma_O,
\end{aligned} \tag{2.3}$$

with given data $\rho_D, \boldsymbol{v}_D, \boldsymbol{z}_D$.

It is easy to see that $\boldsymbol{f}_s(\alpha \boldsymbol{w}) = \alpha\ \boldsymbol{f}_s(\boldsymbol{w})$ for $\alpha > 0$. This property implies that

$$\boldsymbol{f}_s(\boldsymbol{w}) = \mathbb{A}_s(\boldsymbol{w})\boldsymbol{w}, \quad s = 1, 2, \tag{2.4}$$

where $\mathbb{A}_s(\boldsymbol{w}) = D\boldsymbol{f}_s(\boldsymbol{w})/D\boldsymbol{w}$, $s = 1, 2$, are the Jacobi matrices of the mappings $\boldsymbol{f}_s$. The viscous terms $\boldsymbol{R}_s(\boldsymbol{w}, \nabla \boldsymbol{w})$ can be expressed in the form

$$\boldsymbol{R}_s(\boldsymbol{w}, \nabla \boldsymbol{w}) = \sum_{k=1}^{2} \mathbb{K}_{s,k}(\boldsymbol{w}) \frac{\partial \boldsymbol{w}}{\partial x_k}, \quad s = 1, 2, \tag{2.5}$$

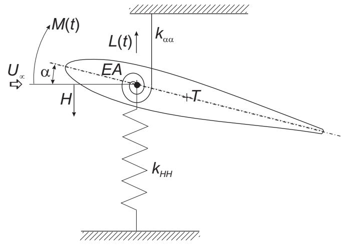

FIG. 3.1. *Elastically supported airfoil with two degrees of freedom.*

where $\mathbb{K}_{s,k}(\boldsymbol{w}) \in I\!R^{4\times 4}$ are matrices depending on $\boldsymbol{w}$ (cf. [3]).

3. Equations for the moving airfoil. The airfoil has two degrees of freedom: the vertical displacement H (positively oriented downwards) and the angle α of rotation around an elastic axis EA (positively oriented clockwise), see Figure 3.1. The motion of the airfoil is described by the system of ordinary differential equations for the unknowns H and α:

$$\begin{aligned} &m\ddot{H} + k_{HH}H + S_\alpha\,\ddot{\alpha}\,\cos\alpha - S_\alpha\dot{\alpha}^2\sin\alpha + d_{HH}\dot{H} = -\mathcal{L}(t), \\ &S_\alpha\ddot{H}\cos\alpha + I_\alpha\ddot{\alpha} + k_{\alpha\alpha}\alpha + d_{\alpha\alpha}\dot{\alpha} = \mathcal{M}(t). \end{aligned} \tag{3.1}$$

The dot and two dots denote the first-order and second-order time derivative, respectively. We use the following notation: $\mathcal{L}(t)$ – aerodynamic lift force (upwards positive), $\mathcal{M}(t)$ – aerodynamic torsional moment (clockwise positive), m - mass of the airfoil, S_α – static moment around the elastic axis EA, I_α – inertia moment around the elastic axis EA, k_{HH} – bending stiffness, $k_{\alpha\alpha}$ – torsional stiffness, d_{HH} – structural damping in bending, $d_{\alpha\alpha}$ – structural damping in torsion, l – airfoil depth.

System (3.1) was derived from the Lagrange equations in [12]. It is equipped with the initial conditions prescribing the values $H(0)$, $\alpha(0)$, $\dot{H}(0)$, $\dot{\alpha}(0)$. The aerodynamic lift force $\mathcal{L}$ acting in the vertical direction and the torsional moment $\mathcal{M}$ are defined by

$$\mathcal{L} = -\,l\int_{\Gamma_{Wt}}\sum_{j=1}^{2}\tau_{2j}n_j\,\mathrm{d}S, \quad \mathcal{M} = l\int_{\Gamma_{Wt}}\sum_{i,j=1}^{2}\tau_{ij}n_j r_i^{\mathrm{ort}}\,\mathrm{d}S, \tag{3.2}$$

where

$$\begin{aligned} &\tau_{ij} = (-p + \lambda\,\mathrm{div}\boldsymbol{v})\delta_{ij} + \mu\Big(\frac{\partial u_i}{\partial x_j} + \frac{\partial u_j}{\partial x_i}\Big), \\ &r_1^{\mathrm{ort}} = -(x_2 - x_{EA2}),\ r_2^{\mathrm{ort}} = x_1 - x_{EA1}, \end{aligned} \tag{3.3}$$

$\boldsymbol{n} = (n_1, n_2)$ is the unit outer normal to $\partial\Omega_t$ on Γ_{Wt}.

4. Space discretization of the flow problem. For the space semidiscretization we use the discontinuous Galerkin finite element method (DGFEM). We construct a polygonal approximation Ω_{ht} of the domain Ω_t. By $\mathcal{T}_{ht}$ we denote a partition of the closure $\overline{\Omega}_{ht}$ of the domain Ω_{ht} into a finite number of closed triangles K with mutually disjoint interiors such that $\overline{\Omega}_{ht} = \bigcup_{K\in\mathcal{T}_{ht}} K$.

By $\mathcal{F}_{ht}$ we denote the system of all faces of all elements $K \in \mathcal{T}_{ht}$. Further, we introduce the set of boundary faces $\mathcal{F}_{ht}^B = \{\Gamma \in \mathcal{F}_{ht};\ \Gamma \subset \partial\Omega_{ht}\}$, the set of "Dirichlet" boundary faces $\mathcal{F}_{ht}^D = \{\Gamma \in \mathcal{F}_{ht}^B;$ a Dirichlet condition is prescribed on $\Gamma\}$ and the set of inner faces $\mathcal{F}_{ht}^I = \mathcal{F}_{ht} \setminus \mathcal{F}_{ht}^B$. Each $\Gamma \in \mathcal{F}_{ht}$ is associated with a unit normal vector $\boldsymbol{n}_\Gamma$ to Γ. For $\Gamma \in \mathcal{F}_{ht}^B$ the normal $\boldsymbol{n}_\Gamma$ has the same orientation as the outer normal to $\partial\Omega_{ht}$. We set $d(\Gamma) =$ length of $\Gamma \in \mathcal{F}_{ht}$ and $h_K =$ diameter of $K \in \mathcal{T}_{ht}$.

For each $\Gamma \in \mathcal{F}_{ht}^I$ there exist two neighbouring elements $K_\Gamma^{(L)}, K_\Gamma^{(R)} \in \mathcal{T}_h$ such that $\Gamma \subset \partial K_\Gamma^{(R)} \cap \partial K_\Gamma^{(L)}$. We use the convention that $K_\Gamma^{(R)}$ lies in the direction of $\boldsymbol{n}_\Gamma$ and $K_\Gamma^{(L)}$ lies in the opposite direction to $\boldsymbol{n}_\Gamma$. If $\Gamma \in \mathcal{F}_{ht}^B$, then the element adjacent to Γ will be denoted by $K_\Gamma^{(L)}$.

The approximate solution will be sought in the space of piecewise polynomial functions $\boldsymbol{S}_{ht} = [S_{ht}]^4 = S_{ht} \times S_{ht} \times S_{ht} \times S_{ht}$ with $S_{ht} = \{v; v|_K \in P_r(K)\ \forall\, K \in \mathcal{T}_{ht}\}$, where $r > 0$ is an integer and $P_r(K)$ denotes the space of all polynomials on K of degree $\leq r$. A function $\boldsymbol{\varphi} \in \boldsymbol{S}_{ht}$ is, in general, discontinuous on interfaces $\Gamma \in \mathcal{F}_{ht}^I$. By $\boldsymbol{\varphi}_\Gamma^{(L)}$ and $\boldsymbol{\varphi}_\Gamma^{(R)}$ we denote the values of $\boldsymbol{\varphi}$ on Γ considered from the interior and the exterior of $K_\Gamma^{(L)}$, respectively, and set $\langle \boldsymbol{\varphi} \rangle_\Gamma = (\boldsymbol{\varphi}_\Gamma^{(L)} + \boldsymbol{\varphi}_\Gamma^{(R)})/2, \quad [\boldsymbol{\varphi}]_\Gamma = \boldsymbol{\varphi}_\Gamma^{(L)} - \boldsymbol{\varphi}_\Gamma^{(R)}$.

The discrete problem is derived in the following way: We multiply system (2.1) by a test function $\boldsymbol{\varphi}_h \in \boldsymbol{S}_{ht}$, integrate over $K \in \mathcal{T}_{ht}$, apply Green's theorem, sum over all elements $K \in \mathcal{T}_{ht}$, use the concept of the numerical flux and introduce suitable terms mutually vanishing for a regular exact solution and linearize the resulting forms on the basis of properties of functions $\boldsymbol{f}_s$ and $\boldsymbol{R}_s$ (see, e.g. [8]). In this way we get the following forms (followed by the explanation of symbols appearing in their definitions):

$$
\begin{aligned}
\hat{a}_h(\overline{\boldsymbol{w}}_h, \boldsymbol{w}_h, \boldsymbol{\varphi}_h, t) = & \sum_{K \in \mathcal{T}_{ht}} \int_K \sum_{s=1}^{2} \sum_{k=1}^{2} \mathbb{K}_{s,k}(\overline{\boldsymbol{w}}_h) \, \frac{\partial \boldsymbol{w}_h}{\partial x_k} \cdot \frac{\partial \boldsymbol{\varphi}_h}{\partial x_s} \, \mathrm{d}\boldsymbol{x} \\
& - \sum_{\Gamma \in \mathcal{F}_{ht}^I} \int_\Gamma \sum_{s=1}^{2} \left\langle \sum_{k=1}^{2} \mathbb{K}_{s,k}(\overline{\boldsymbol{w}}_h) \frac{\partial \boldsymbol{w}_h}{\partial x_k} \right\rangle (\boldsymbol{n}_\Gamma)_s \cdot [\boldsymbol{\varphi}_h] \, \mathrm{d}S \\
& - \sum_{\Gamma \in \mathcal{F}_{ht}^D} \int_\Gamma \sum_{s=1}^{2} \sum_{k=1}^{2} \mathbb{K}_{s,k}(\overline{\boldsymbol{w}}_h) \frac{\partial \boldsymbol{w}_h}{\partial x_k} (\boldsymbol{n}_\Gamma)_s \cdot \boldsymbol{\varphi}_h \, \mathrm{d}S \\
& - \Theta \sum_{\Gamma \in \mathcal{F}_{ht}^I} \int_\Gamma \sum_{s=1}^{2} \left\langle \sum_{k=1}^{2} \mathbb{K}_{k,s}^T(\overline{\boldsymbol{w}}_h) \frac{\partial \boldsymbol{\varphi}_h}{\partial x_k} \right\rangle (\boldsymbol{n}_\Gamma)_s \cdot [\boldsymbol{w}_h] \, \mathrm{d}S \\
& - \Theta \sum_{\Gamma \in \mathcal{F}_{ht}^D} \int_\Gamma \sum_{s=1}^{2} \sum_{k=1}^{2} \mathbb{K}_{k,s}^T(\overline{\boldsymbol{w}}_h) \frac{\partial \boldsymbol{\varphi}_h}{\partial x_k} (\boldsymbol{n}_\Gamma)_s \cdot \boldsymbol{w}_h \, \mathrm{d}S,
\end{aligned}
\tag{4.1}
$$

$$
J_h(\boldsymbol{w}_h, \boldsymbol{\varphi}_h, t) = \sum_{\Gamma \in \mathcal{F}_{ht}^I} \int_\Gamma \sigma [\boldsymbol{w}_h] \cdot [\boldsymbol{\varphi}_h] \, \mathrm{d}S + \sum_{\Gamma \in \mathcal{F}_{ht}^D} \int_\Gamma \sigma \boldsymbol{w}_h \cdot \boldsymbol{\varphi}_h \, \mathrm{d}S, \tag{4.2}
$$

$$
\begin{aligned}
\ell_h(\boldsymbol{w}_h, \boldsymbol{\varphi}_h, t) = & \sum_{\Gamma \in \mathcal{F}_{ht}^D} \int_\Gamma \sum_{s=1}^{2} \sigma \boldsymbol{w}_B \cdot \boldsymbol{\varphi}_h \, \mathrm{d}S \\
& - \Theta \sum_{\Gamma \in \mathcal{F}_{ht}^D} \int_\Gamma \sum_{s=1}^{2} \sum_{k=1}^{2} \mathbb{K}_{k,s}^T(\overline{\boldsymbol{w}}_h) \frac{\partial \boldsymbol{\varphi}_h}{\partial x_k} (\boldsymbol{n}_\Gamma)_s \cdot \boldsymbol{w}_B \, \mathrm{d}S,
\end{aligned}
\tag{4.3}
$$

$$d_h(\boldsymbol{w}_h, \boldsymbol{\varphi}_h, t) = \sum_{K\in\mathcal{T}_{ht}} \int_K (\boldsymbol{w}_h \cdot \boldsymbol{\varphi}_h)\,\mathrm{div}\boldsymbol{z}\,\mathrm{d}x. \tag{4.4}$$

$$\begin{aligned}
&\hat{b}_h(\overline{\boldsymbol{w}}_h, \boldsymbol{w}_h, \boldsymbol{\varphi}_h, t) \qquad\qquad (4.5)\\
&= -\sum_{K\in\mathcal{T}_{ht}} \int_K \sum_{s=1}^{2} (\mathbb{A}_s(\overline{\boldsymbol{w}}_h(x)) - z_s(x))\mathbb{I})\boldsymbol{w}_h(x))\cdot \frac{\partial \boldsymbol{\varphi}_h(x)}{\partial x_s} dx\\
&+ \sum_{\Gamma\in\mathcal{F}^I_{ht}} \int_\Gamma \Big(\mathbb{P}^+_g(\langle\overline{\boldsymbol{w}}_h\rangle_\Gamma, \boldsymbol{n}_\Gamma)\boldsymbol{w}_h^{(L)} + \mathbb{P}^-_g(\langle\overline{\boldsymbol{w}}_h\rangle_\Gamma, \boldsymbol{n}_\Gamma)\boldsymbol{w}_h^{(R)}\Big)\cdot [\boldsymbol{\varphi}_h]\,\mathrm{d}S\\
&+ \sum_{\Gamma\in\mathcal{F}^B_{ht}} \int_\Gamma \Big(\mathbb{P}^+_g(\langle\overline{\boldsymbol{w}}_h\rangle_\Gamma, \boldsymbol{n}_\Gamma)\boldsymbol{w}_h^{(L)} + \mathbb{P}^-_g(\langle\overline{\boldsymbol{w}}_h\rangle_\Gamma, \boldsymbol{n}_\Gamma)\overline{\boldsymbol{w}}_h^{(R)}\Big)\cdot \boldsymbol{\varphi}_h\,\mathrm{d}S,
\end{aligned}$$

We set $\Theta = 1$ or $\Theta = 0$ or $\Theta = -1$ and get the so-called symmetric version (SIPG) or incomplete version (IIPG) or nonsymmetric version (NIPG), respectively, of the discretization of viscous terms. The symbols $\mathbb{P}^+(\boldsymbol{w}, \boldsymbol{n})$ and $\mathbb{P}^-(\boldsymbol{w}, \boldsymbol{n})$ denote the positive and negative part of the matrix $\mathbb{P}(\boldsymbol{w}, \boldsymbol{n}) = \sum_{s=1}^{2}(\mathbb{A}_s(\boldsymbol{w}) - z_s\mathbb{I})n_s$ defined similarly as in [9]. In (4.2), $\sigma|_\Gamma = C_W\mu/d(\Gamma)$ and $C_W > 0$ is a sufficiently large constant. The boundary state $\boldsymbol{w}_B$ is defined on the basis of the Dirichlet boundary conditions (2.3), a), b), d) and extrapolation:

$$\boldsymbol{w}_B = (\rho_D, \rho_D v_{D1}, \rho_D v_{D2}, c_v\rho_D\theta_\Gamma^{(L)} + \frac{1}{2}\rho_D|\boldsymbol{v}_D|^2) \quad \text{on } \Gamma_I, \tag{4.6}$$

$$\boldsymbol{w}_B = \boldsymbol{w}_\Gamma^{(L)} \quad \text{on } \Gamma_O, \tag{4.7}$$

$$\boldsymbol{w}_B = (\rho_\Gamma^{(L)}, \rho_\Gamma^{(L)} z_{D1}, \rho_\Gamma^{(L)} z_{D2}, c_v\rho_\Gamma^{(L)}\theta_\Gamma^{(L)} + \frac{1}{2}\rho_\Gamma^{(L)}|\boldsymbol{z}_D|^2) \quad \text{on } \Gamma_{W_t}. \tag{4.8}$$

For $\Gamma \in \mathcal{F}^B_{ht}$ we set $\langle\overline{\boldsymbol{w}}_h\rangle_\Gamma = (\overline{\boldsymbol{w}}_\Gamma^{(L)} + \overline{\boldsymbol{w}}_\Gamma^{(R)})/2$ and the boundary state $\overline{\boldsymbol{w}}_\Gamma^{(R)}$ is defined with the aid of the solution of the 1D linearized initial-boundary Riemann problem as in [6].

In order to avoid spurious oscillations in the approximate solution in the vicinity of discontinuities or steep gradients, we apply local artificial viscosity forms. They are based on the discontinuity indicator $g_t(K) = \int_{\partial K}[\overline{\rho}_h]^2\,\mathrm{d}S/(h_K|K|^{3/4}),\quad K \in \mathcal{T}_{ht}$, introduced in [4]. By $[\overline{\rho}_h]$ we denote the jump of the function $\overline{\rho}_h$ on the boundary ∂K and $|K|$ denotes the area of the element K. Then we define the discrete discontinuity indicator $G_t(K) = 0$ if $g_t(K) < 1$, $G_t(K) = 1$ if $g_t(K) \geq 1$, and the artificial viscosity forms (see [9])

$$\hat{\beta}_h(\overline{\boldsymbol{w}}_h, \boldsymbol{w}_h, \boldsymbol{\varphi}_h, t) = \nu_1 \sum_{K\in\mathcal{T}_{ht}} h_K G_t(K) \int_K \nabla\boldsymbol{w}_h\cdot\nabla\boldsymbol{\varphi}_h\,\mathrm{d}\boldsymbol{x}, \tag{4.9}$$

$$\hat{J}_h(\overline{\boldsymbol{w}}_h, \boldsymbol{w}_h, \boldsymbol{\varphi}_h, t) = \nu_2 \sum_{\Gamma\in\mathcal{F}^I_{ht}} \frac{1}{2}\big(G_t(K_\Gamma^{(L)}) + G_t(K_\Gamma^{(R)})\big)\int_\Gamma [\boldsymbol{w}_h]\cdot[\boldsymbol{\varphi}_h]\,\mathrm{d}S,$$

with parameters ν_1, $\nu_2 = O(1)$.

In order to increase the quality of the numerical approximations, in [2], isoparametric elements were used.

4.1. Time discretization by the BDF method. Let us construct a partition $0 = t_0 < t_1 < t_2 \ldots$ of the time interval $[0, T]$ and define the time step $\tau_n = t_n - t_{n-1}$. We use the approximations $\boldsymbol{w}_h(t_n) \approx \boldsymbol{w}_h^n \in \boldsymbol{S}_{ht_n}$, $\boldsymbol{z}(t_n) \approx \boldsymbol{z}^n$, $n = 0, 1, \ldots$. Let

TABLE 4.1
The coefficients α_l.

	$q=1$	$q=2$	$q=3$
α_0	$\frac{1}{\tau_m}$,	$\frac{2\tau_m+\tau_{m-1}}{\tau_m(\tau_m+\tau_{m-1})}$,	$\frac{(2\tau_m+\tau_{m-1})(2\tau_m+\tau_{m-1}+\tau_{m-2})-\tau_m^2}{\tau_m(\tau_m+\tau_{m-1})(\tau_m+\tau_{m-1}+\tau_{m-2})}$
α_1	$-\frac{1}{\tau_m}$,	$-\frac{\tau_m+\tau_{m-1}}{\tau_m\tau_{m-1}}$,	$-\frac{(\tau_m+\tau_{m-1})(\tau_m+\tau_{m-1}+\tau_{m-2})}{\tau_m\tau_{m-1}(\tau_{m-1}+\tau_{m-2})}$
α_2		$\frac{\tau_m}{\tau_{m-1}(\tau_m+\tau_{m-1})}$,	$\frac{\tau_m(\tau_m+\tau_{m-1}+\tau_{m-2})}{\tau_{m-1}\tau_{m-2}(\tau_m+\tau_{m-1})}$
α_3			$-\frac{\tau_m(\tau_m+\tau_{m-1})}{\tau_{m-2}(\tau_m+\tau_{m-1}+\tau_{m-2})(\tau_{m-1}+\tau_{m-2})}$

TABLE 4.2
The coefficients β_l.

	$q=1$	$q=2$	$q=3$
β_1	1,	$\frac{\tau_m+\tau_{m-1}}{\tau_{m-1}}$,	$\frac{(\tau_m+\tau_{m-1}+\tau_{m-2})(\tau_m+\tau_{m-1})}{\tau_{m-1}(\tau_{m-1}+\tau_{m-2})}$
β_2		$-\frac{\tau_m}{\tau_{m-1}}$,	$-\frac{\tau_m(\tau_m+\tau_{m-1}+\tau_{m-2})}{\tau_{m-1}\tau_{m-2}}$
β_3			$\frac{\tau_m(\tau_m+\tau_{m-1})}{\tau_{m-2}(\tau_{m-1}+\tau_{m-2})}$

us assume that $\boldsymbol{w}_h^n,\ n=0,\dots,m-1$, are already known. Then we introduce the functions $\hat{\boldsymbol{w}}_h^n = \boldsymbol{w}_h^n \circ \mathcal{A}_{t_n} \circ \mathcal{A}_{t_m}^{-1}$ for $n = m-1, m-2, \dots$, which are defined in the domain Ω_{ht_m}. The ALE derivative at time t_m is approximated by the backward finite difference formula (BDF) of order q:

$$\frac{D^{\mathcal{A}}\boldsymbol{w}_h}{Dt}(t_m) \approx \frac{D^{\mathcal{A}}_{appr}\boldsymbol{w}_h}{Dt}(t_m) = \alpha_0 \boldsymbol{w}_h^m + \sum_{l=1}^{q} \alpha_l \hat{\boldsymbol{w}}_h^{m-l},$$

with coefficients $\alpha_l,\ l=0,...,q$, depending on $\tau_{m-l},\ l=0,...,q-1$. In the begining of the computation, when $m<q$, we approximate the ALE derivative by formulas of the lower order $q:=m$. In nonlinear terms we use the extrapolation for the computation of the state $\overline{\boldsymbol{w}}_h^m$:

$$\overline{\boldsymbol{w}}_h^m = \sum_{l=1}^{q} \beta_l \hat{\boldsymbol{w}}_h^{m-l}, \tag{4.10}$$

where $\beta_l,\ l=1,...,q$, depend on $\tau_{m-l},\ l=0,...,q-1$. If $m<q$, then we apply the extrapolation of order m. The values of the coefficients $\alpha_l, l=0,...,q$, and $\beta_l, l=1,...,q$, for $q=1,2,3$ are given in Tables 4.1 and 4.2, respectively.

By the symbol $(\cdot,\cdot)_{t_m}$ we shall denote the scalar product in $L^2(\Omega_{ht_m})$, i.e.

$$(\boldsymbol{w}_h, \boldsymbol{\varphi}_h)_{t_m} = \int_{\Omega_{ht_m}} \boldsymbol{w}_h \cdot \boldsymbol{\varphi}_h \, dx. \tag{4.11}$$

The resulting *BDF-DG scheme* has the following form: For each $m = 1, 2, \ldots$ we seek $\boldsymbol{w}_h^m \in \boldsymbol{S}_{ht_m}$ such that

$$\begin{aligned}
&\left(\frac{D^{\mathcal{A}}_{appr} \boldsymbol{w}_h}{Dt}(t_m), \boldsymbol{\varphi}_h \right)_{t_m} + \hat{b}_h(\overline{\boldsymbol{w}}_h^m, \boldsymbol{w}_h^m, \boldsymbol{\varphi}_h, t_m) + \hat{a}_h(\overline{\boldsymbol{w}}_h^m, \boldsymbol{w}_h^m, \boldsymbol{\varphi}_h, t_m) \\
&+ J_h(\boldsymbol{w}_h^m, \boldsymbol{\varphi}_h, t_m) + d_h(\boldsymbol{w}_h^m, \boldsymbol{\varphi}_h, t_m) + \hat{\beta}_h(\overline{\boldsymbol{w}}_h^m, \boldsymbol{w}_h^m, \boldsymbol{\varphi}_h, t_m) \\
&+ \hat{J}_h(\overline{\boldsymbol{w}}_h^m, \boldsymbol{w}_h^m, \boldsymbol{\varphi}_h, t_m) = \ell(\overline{\boldsymbol{w}}_B^m, \boldsymbol{\varphi}_h, t_m), \quad \forall \boldsymbol{\varphi}_h \in \boldsymbol{S}_{ht_m}.
\end{aligned} \tag{4.12}$$

The numerical solution of the structural problem, in contrast to the solution of the compressible flow, is not difficult. System (3.1) is transformed to a first-order system and approximated by the Runge-Kutta method. In what follows, we shall be concerned with the realization of the complete fluid-structure interaction problem.

4.2. Construction of the ALE mapping. There exist various possibilities how to construct the ALE mapping $\mathcal{A}_t$. In the case of flow past an isolated airfoil it is possible to use the procedure introduced in [2]. We start from the assumption that we know the airfoil position at time instants t_m, given by the displacement $H(t_m)$ and rotation angle $\alpha(t_m)$ and want to define the mapping $\mathcal{A}_{t_m} : \overline{\Omega}_{h0} \to \overline{\Omega}_{ht_m}$ We construct two circles K_1, K_2 with center at the elastic axis EA and radii $R_1, R_2,\ 0 < R_1 < R_2$ so that the airfoil is lying inside the circle K_1. The interior of the circle K_1 is moving in the vertical direction and rotates around the elastic axis as a solid body together with the airfoil. The exterior of K_2 is not deformed and in the area between K_1 and K_2 we use the intepolation. First we define the mapping $\mathbf{H}_{t_m}(X_1, X_2)$, where $\boldsymbol{X} = (X_1, X_2) \in \Omega_{h0}$, describing the vertical motion and rotation:

$$\begin{aligned}
\mathbf{H}_{t_m}(X_1, X_2) = &\begin{pmatrix} \cos\alpha(t_m) & \sin\alpha(t_m) \\ -\sin\alpha(t_m) & \cos\alpha(t_m) \end{pmatrix} \begin{pmatrix} X_1 - X_{EA1} \\ X_2 - X_{EA2} \end{pmatrix} \\
&+ \begin{pmatrix} X_{EA1} \\ X_{EA2} \end{pmatrix} + \begin{pmatrix} 0 \\ -H(t_m) \end{pmatrix},
\end{aligned} \tag{4.13}$$

where (X_{EA1}, X_{EA2}) represents the position of the elastic axis at time $t = 0$. If we denote the identical mapping by $\mathbf{Id}(X_1, X_2) = (X_1, X_2)$, we define the mapping $\overline{\mathcal{A}}_{t_m}$ as a combination of $\mathbf{Id}$ and $\mathbf{H}_{t_m}$:

$$\bar{\mathcal{A}}_{t_m}(X_1, X_2) = (1 - \xi)\mathbf{H}_{t_m}(X_1, X_2) + \xi \mathbf{Id}(X_1, X_2), \tag{4.14}$$

where

$$\xi = \xi(\hat{r}) = \min\left(\max\left(0, \frac{\hat{r} - R_1}{R_2 - R_1} \right), 1 \right) \tag{4.15}$$

and $\hat{r} = \sqrt{(X_1 - X_{EA1})^2 + (X_2 - X_{EA2})^2}$ is the distance of a point $\boldsymbol{X} \in \Omega_{h0}$ from the elastic axis. Finally, the ALE mapping $\mathcal{A}_t$ is defined as the conforming piecewise linear interpolation of $\bar{\mathcal{A}}_t$.

The domain velocity is approximated by the formula of order q in the form

$$\boldsymbol{z}^m(\boldsymbol{x}) = \alpha_0 \boldsymbol{x} + \sum_{l=1}^{q} \alpha_l \mathcal{A}_{t_{m-l}}(\mathcal{A}_{t_m}^{-1}(\boldsymbol{x})) \quad \text{for } \boldsymbol{x} \in \Omega_{ht_m}, \tag{4.16}$$

with coefficients $\alpha_l, l = 0, ..., q$, given in Table 4.1. If $m < q$, then we set $q := m$.

4.3. Coupling procedure. In the solution of the complete coupled fluid-structure interaction problem it is necessary to apply a suitable coupling procedure. Here we apply the following algorithm.

0. Prescribe $\varepsilon > 0$ - the measure of accuracy in the coupling procedure, and an integer $N \geq 0$ - the maximal number of iterations in the coupling procedure.
1. Assume that the approximate solution $\boldsymbol{w}_h^{m-1}$ of the discrete flow problem (4.12) and the corresponding lift force $\mathcal{L}$ and torsional moment $\mathcal{M}$ computed from (3.2) - (3.3) are known.
2. Extrapolate linearly $\mathcal{L}$ and $\mathcal{M}$ from the interval $[t_{m-2}, t_{m-1}]$ to $[t_{m-1}, t_m]$. Set $n := 0$.
3. *Prediction of* H, α: Compute the displacement H and angle α at time t_m as the solution of system (3.1). Denote it by H^*, α^*.
4. On the basis of H^*, α^* determine the position of the airfoil at time t_m, the domain Ω_{ht_m}, the ALE mapping $\mathcal{A}_{ht_m}$ and the domain velocity $\boldsymbol{z}_h^m$.
5. Solve the discrete problem (4.12) at time t_m.
6. *Correction of* H, α: Compute $\mathcal{L}$, $\mathcal{M}$ from (3.2) - (3.3) at time t_m and interpolate $\mathcal{L}$, $\mathcal{M}$ in the interval $[t_{m-1}, t_m]$. Compute h, α at time t_m from (3.1).
7. If $|H^* - H| + |\alpha^* - \alpha| \geq \varepsilon$ and $n < N$, set $H^* = H$, $\alpha^* = \alpha$, $n := n + 1$ and go to 4. Otherwise, $m := m + 1$ and go to 2.

If $N = 0$, then we get a weak (loose) coupling of the flow and structural problems. With increasing N and decreasing ε, the coupling becomes stronger.

5. Numerical experiments. In order to demonstrate the applicability and robustness of the developed method, numerical tests were performed. Here we present the results of computations carried out with the following data: $m = 0.086622$ kg, $S_\alpha = -0.000779673$ kg m, $I_\alpha = 0.000487291$ kg m^2, $k_{HH} = 105.109$ N m^{-1}, $k_{\alpha\alpha} = 3.696682$ N m rad^{-1}, $l = 0.05$ m, $c = 0.3$ m, $\mu = 1.8375 \cdot 10^{-5}$ kg m^{-1} s^{-1}, far-field density $\rho = 1.225$ kg m^{-3}, $H(0) = 0.02$ m, $\alpha(0) = 6$ degrees, $\dot{H}(0) = 0, \dot{\alpha} = 0$. We neglect the structural damping. The elastic axis is placed on the airfoil chord at the 40% distance from the leading edge.

For the space discretization quadratic polynomials ($r = 2$) were used and the time discretization was carried out by the second-order BDF method ($q = 2$). The discretization of the viscous terms was realized by the SIPG version. The parameter $C_W = 500$ in the interior part of the penalty form J_h was used, whereas in the boundary penalty $C_W = 5000$. The constants in the artificial viscosity forms were chosen $\nu_1 = \nu_2 = 0.1$.

The computational process starts at time $t = -\delta < 0$ by the solution of the flow, keeping the airfoil in a fixed position given by the prescribed initial translation H and the angle of attack α. Then, at time $t = 0$ the airfoil is released and we continue by the solution of a complete fluid-structure interaction problem.

Figure 5.1 shows the displacement H and the rotation angle α in dependence on time for the far-field velocity 30 and 40 m s^{-1}. The corresponding Reynolds numbers

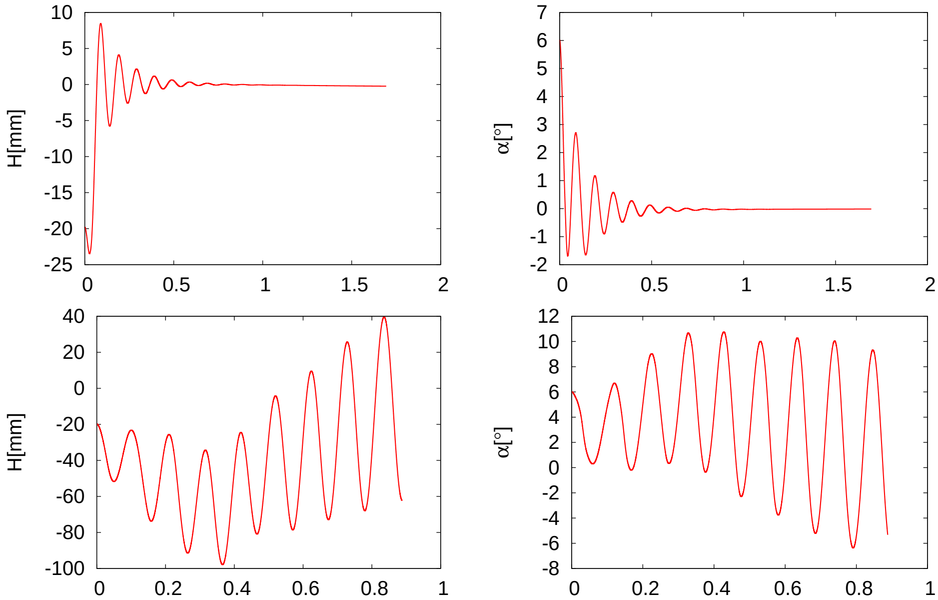

FIG. 5.1. *Displacement H (left) and rotation angle α (right) of the airfoil in dependence on time for far-field velocity 30 and 40 $\mathrm{m\,s^{-1}}$.*

are $6 \cdot 10^5$ and $8 \cdot 10^5$, respectively. We see that for the velocity 30 $\mathrm{m\,s^{-1}}$ the vibrations are damped, but for the velocity 40 $\mathrm{m\,s^{-1}}$ we get the flutter instability, when the vibration amplitudes are increasing in time.

The developed method also allows the numerical simulation of airfoil vibrations induced by high-speed transonic or hypersonic flow. Here we present the results of the simulation of airfoil vibrations induced by the flow with far-field Mach number $M_\infty = 1.2$ and Reynolds number $Re = 10^4$. In this case damped airfoil vibrations were obtained for the same data as above except the bending and torsional stiffnesses, which were now 1000 times higher than before. Figure 5.2 shows Mach number distribution in the vicinity of the airfoil at several time instants. One can see well resolved obligue shock wave, shock waves leaving the trailing edge and wake.

6. Conclusion . The paper is concerned with the development and applications of the numerical method for the simulation of airfoil vibrations induced by viscous compressible flow. The gas flow is described by the 2D compressible Navier-Stokes equations in the ALE formulation allowing to take into account time dependence of the computational domain. The flow problem is coupled with the structural problem represented by the system of second-order ordinary differential equations for the vertical displacement and torsional angle of the airfoil. For the discretization of the flow problem the space DGFEM combined with the BDF time discretization was applied. This method is coupled with the Runge-Kutta method for the solution of the system of ordinary differential equations describing the airfoil vibrations. Numerical experiments show that the method can be applied to the simulation of airfoil vibrations induced by compressible subsonic as well as transonic flow.

There are the following subjects for further work: realization of further tests of the developed technique, solution of problems with large vibrations, comparison of

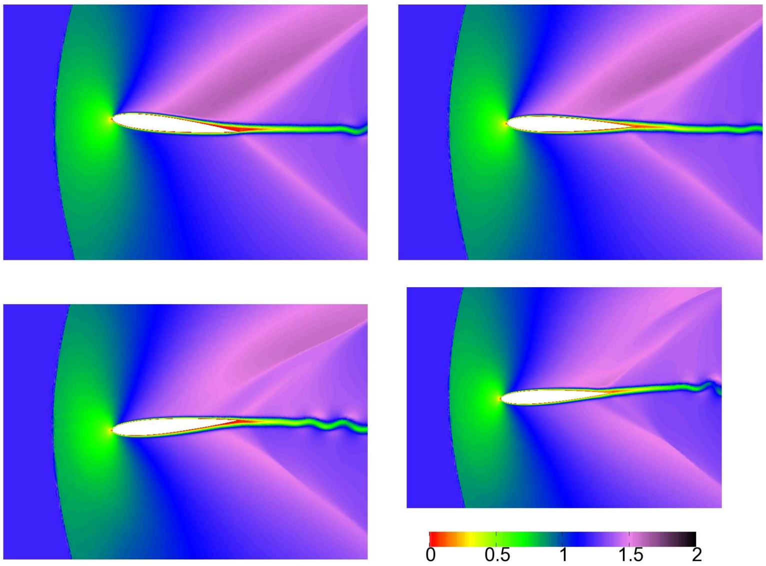

FIG. 5.2. *Mach number distribution at time instants t = 0.0 s, 0.00049 s, 0.00098 s, 0.00147 s, for far-field velocity 408 m s^{-1}, Mach number Ma = 1.2 and Reynolds number Re = 10^4.*

obtained results with wind tunnel experiments, and theoretical analysis of qualitative properties (as, e.g. stability, convergence) of the developed numerical method.

REFERENCES

[1] R.L. Bisplinghoff, H. Ashley, and R.L. Halfman, *Aeroelasticity*, Dover, New York, 1996.
[2] J. Česenek, *Discontinuous Galerkin method for the solution of compressible viscous flow*, Charles University in Prague, Faculty of Mathematics and Physics, 2011 (in Czech).
[3] V. Dolejší, *Semi-implicit interior penalty discontinuous Galerkin methods for viscous compressible flows*, Commun. Comput. Phys., 4 (2008), pp. 231–274.
[4] V. Dolejší, M. Feistauer, and C. Schwab, *On some aspects of the discontinuous Galerkin finite element method for conservation laws*, Math. Comput. Simul., 61 (2003), pp. 333–346.
[5] E.H.Dowell, *A Modern Course in Aeroelasticity*, Kluwer, Dodrecht, 1995.
[6] M. Feistauer, J. Česenek, J. Horáček, V. Kučera, and J. Prokopová, *DGFEM for the numerical solution of compressible flow in time dependent domains and applications to fluid-structure interaction*, Proceedings of the 5th European Conference on Computational Fluid Dynamics ECCOMAS CFD 2010, J.C.F. Pereira and A. Sequeira (Eds), Lisbon, Portugal, 14-17 June 2010 (published ellectronically), ISBN 978-989-96778-1-4.
[7] M. Feistauer, J. Felcman, and I. Straškraba, *Mathematical and Computational Methods for Compressible Flow*, Clarendon Press, Oxford, 2003.
[8] M. Feistauer, J. Horáček, V. Kučera, and J. Prokopová, *On numerical solution of compressible flow in time-dependent domains*, Mathematica Bohemica, 137 (2012), pp. 1–16.
[9] M. Feistauer and V. Kučera, *On a robust discontinuous Galerkin technique for the solution of compressible flow*, J. Comput. Phys., 224 (2007), pp. 208–221.
[10] E.Naudasher, D.Rockwell, *Flow-Induced Vibrations*, A.A. Balkema, Rotterdam, 1994.
[11] T. Nomura, T.J.R. Hughes, *An arbitrary Lagrangian-Eulerian finite element method for interaction of fluid and a rigid body*, Computer Methods in Applied Mechanics and Engineering, 95 (1992), pp. 115-138.
[12] P. Sváček, M. Feistauer, J. Horáček, *Numerical simulation of flow induced airfoil vibrations with large amplitudes*, Journal of Fluids and Structures, 23 (2007), pp. 391–411.